

Electrospun Al-MOF fibers as D4 Siloxane adsorbent: Synthesis, environmental impacts, and adsorption behavior

S. Pioquinto-García, J.R. Álvarez, A.A. Rico-Barragán, Sylvain Giraudet, J.M. Rosas-Martínez, M. Loredo-Cancino, E. Soto-Regalado, V.M. Ovando-Medina, T. Cordero, J. Rodríguez-Mirasol, et al.

▶ **To cite this version:**

S. Pioquinto-García, J.R. Álvarez, A.A. Rico-Barragán, Sylvain Giraudet, J.M. Rosas-Martínez, et al.. Electrospun Al-MOF fibers as D4 Siloxane adsorbent: Synthesis, environmental impacts, and adsorption behavior. Microporous and Mesoporous Materials, 2023, 348, pp.112327. 10.1016/j.micromeso.2022.112327 . hal-03932166

HAL Id: hal-03932166
https://hal.science/hal-03932166

Submitted on 25 Jan 2023

HAL is a multi-disciplinary open access archive for the deposit and dissemination of scientific research documents, whether they are published or not. The documents may come from teaching and research institutions in France or abroad, or from public or private research centers.

L'archive ouverte pluridisciplinaire **HAL**, est destinée au dépôt et à la diffusion de documents scientifiques de niveau recherche, publiés ou non, émanant des établissements d'enseignement et de recherche français ou étrangers, des laboratoires publics ou privés.



Distributed under a Creative Commons Attribution - NonCommercial 4.0 International License

Electrospun Al-MOF Fibers as D4 Siloxane Adsorbent: Synthesis, Environmental Impacts, and Adsorption Behavior.

Sandra Pioquinto-García,[†] J. Raziel Álvarez,[†] Alan A. Rico-Barragán,[†] Sylvain Giraudet,[‡] Juana María Rosas-Martínez,[§] Margarita Loredo-Cancino,[†] Eduardo Soto-Regalado,[§] Tomás Cordero,[§] José Rodríguez-Mirasol[§] and Nancy E. Dávila-Guzmán*[†]*

[†] Facultad de Ciencias Químicas, Universidad Autónoma de Nuevo León, UANL, Av. Universidad S/N, Cd. Universitaria, San Nicolás de los Garza, Nuevo León 66455, Mexico

[‡] Ecole Nationale Supérieure de Chimie de Rennes, 11 Allée de Beaulieu, 35708 Rennes, France

[§]Departamento de Ingeniería Química, Universidad de Málaga, Andalucia Tech., Campus de Teatinos s/n, 29010, Málaga, Spain

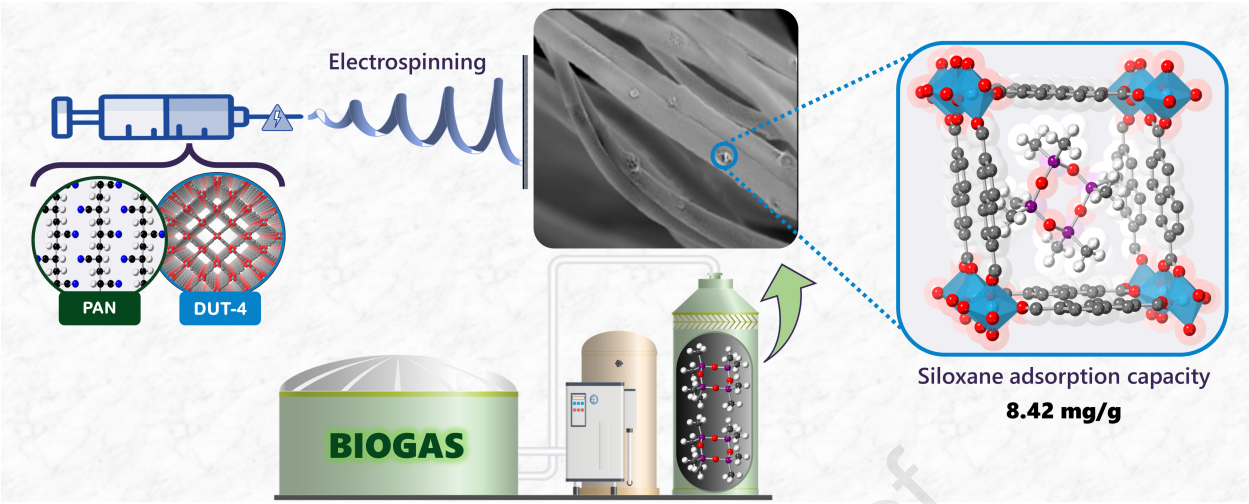
Contact information for the corresponding author (*)

Nancy Elizabeth Dávila-Guzmán, Ph. D.

Universidad Autónoma de Nuevo León

Email: nancy.davilagz@uanl.edu.mx

Journal Pre-proof



Journal Pre-proof

Journal Pre-proof

ABSTRACT

Here, we unveil the great potential of metal-organic framework (MOF) composite fibers produced by the electrospinning method to remove D4 siloxane from gaseous solutions. The fibers are based on polyacrylonitrile (PAN) and a microporous aluminum-based MOF known as DUT-4. The electrospinning configuration and DUT-4:PAN ratio in the precursor solutions play an important role in the textural properties of the fibers. Characterizations of morphology and textural properties demonstrated that the best dispersion on the fiber surface was achieved using coaxial electrospinning with a relationship of 1:1.4 of DUT-4:PAN. The Al-MOF fiber composite was evaluated as a D4 siloxane adsorbent, reaching over 85% of the D4 siloxane uptake capacity of individual DUT-4 crystals but with faster adsorption kinetics (effective diffusion coefficient 3.31 times higher). In addition, the synthesis of the composite showed a lower environmental impact and better thermal stability than that observed for DUT-4. This work shows the novel DUT-4 fibers have an outstanding potential for siloxane removal from biogas streams.

Keywords: Electrospun, metal-organic frameworks, biogas, octamethylcyclotetrasiloxane

1. Introduction

The negotiations to reduce the risks and the impacts of global climate change began in 1988 with the creation of the Intergovernmental Panel on Climate Change (IPCC) under the auspices of the World Meteorological Organization (WMO) and the United Nations. Nowadays, each country voluntarily determines what measures are willing to take against climate change and announces them to the rest of the world at the Conference of the Parties

(COP).[1] Following the line of sustainable development, the transition from fossil fuels to non-conventional energies (*e.g.*, wind, solar, wave, tidal, or biomass) has been promoted worldwide. One type of renewable energy widely spread is biogas, which can be generated for the anaerobic degradation of residual organic materials by the activity of microorganisms.[2]

The biogas is a mixture of methane (55-70%), carbon dioxide (30-45%), moisture, hydrogen sulfide, and volatile organic compounds (VOCs), which may be present in small amounts.[3] Siloxanes can also be formed during the anaerobic fermentation of sewage sludge and organic waste.[4] Siloxanes are a group of Si-based impurities that are considered essential pollutants to remove from biogas.[5] The most abundant siloxanes in biogas are hexamethyldisiloxane (L2), octamethyltrisiloxane (L3), and octamethylcyclotetrasiloxane (D4).[6] They adversely affect biogas combustion systems because they are converted mainly into formaldehyde (CH_2O) and orthosilicic acid (H_4SiO_4), both chemical reagents contribute to abrasion, metal friction, and component failures in machinery.[7]

The concentration of siloxanes in biogas from landfills and wastewater treatment plants covers a wide range between 10 mg m^{-3} and a maximum value of up to 2,000 mg m^{-3}.[8] There is no standard specifying the maximum concentration of siloxanes in biogas, but a standard general limit of 15 mg m^{-3} is recommended.[9] The necessity to remove siloxane from biogas is also a priority in order to enhance biogas' energy recovery potential. Current technologies for siloxane removal from biogas include adsorption, absorption, cryogenics, separation by membranes, and biological processes.[10] However, solid-gas adsorption

63 technology has a huge potential due to its low cost, high selectivity, and simple
64 operation.[11]

65 Although solid adsorbents such as activated carbon (AC) or zeolites have been used for
66 siloxane removal, metal-organic frameworks (MOFs) remain promising candidates for this
67 challenging task.[12] MOFs are porous crystalline structures of metal groups joined
68 together by organic ligands. They have high selectivity and feasible recycling/regeneration
69 for biogas purification,[13] mainly due to their large surface area and versatile tunability of
70 their pore environments.[14–16] However, there is still a lack of research attention on using
71 MOFs as platforms for siloxane removal.[17]

72 Mito-oka and coworkers [12] employed three different microporous compounds for
73 siloxane, including DUT-4 (DUT = Dresden University of Technology). DUT-4 is a 3D
74 aluminum-based MOF constructed from a rigid linear 2,6-naphthalenedicarboxylate (2,6-
75 NDC) ligand (Fig. 1). This MOF has the empirical formula $C_{48}H_{28}O_{20}Al_4$, crystallizes in
76 the orthorhombic space group *Pnna.*[18] Its hydrophobic behavior and large BET surface
77 area make DUT-4 an ideal choice for siloxane removal, with a maximum adsorption
78 capacity of 0.5 g g^{-1}.[17] Nevertheless, its poor thermo-mechanical stability, like many
79 other MOFs, is the main obstacle for any real large-scale application. To overcome this
80 problem, several supports have been employed to immobilize powder MOFs with small
81 particle sizes,[19] among which fibers have stood out due to their remarkable properties. In
82 fact, several previous studies have revealed that fibrous structures facilitate the adsorption
83 or catalytic processes.[20–22]

Journal Pre-proof

Despite all the possible methods currently available for the fabrication of complex fibers, the electrospinning technique remains a simple, versatile, and cost-effective method to manufacture them.[23] Ostermann *et al.* [24] prepared fibers of MOF for the first time by electrospinning, obtaining a hierarchical MOF fiber with a high surface area and easy accessibility. On top of that, the thermal decomposition temperature was enhanced after incorporating the electrospun fibers in a Cr-MOF.[25] Bearing these considerations in mind, functionalized fibers with MOF could be a viable option to remove siloxanes because of their selectivity in wet conditions, renewability at low temperatures (< 300 ºC), and reusability. However, to the best of our knowledge, studies of electrospun fibers for applications in biogas purification processes using MOF have not been reported before. For this reason, the present work presents the preparation of DUT-4 electrospun fibers by dissolution methods to improve their adsorption properties of siloxane D4.

2. Materials and methods

2.1. Preparation of electrospun solutions

The Al-MOF fibers were prepared using DUT-4, *N*, *N*-dimethylformamide (DMF), and polyacrylonitrile (PAN, $M_w \sim 150{,}000$ g/mol) solutions. DUT-4 was synthesized according to the procedures previously described [26]; DMF and PAN were purchased from Sigma-Aldrich and used as received without further purification. The solutions were sonicated for up to 4 h to obtain a homogeneous DUT-4 dispersion on the surface of electrospun fibers and MOF particles smaller than 100 nm. The homogeneous suspensions for uniaxial electrospinning were composed of solutions 1 and 2 (see Table 1). Previously, each solution was prepared at 350 rpm for about 1 h but held at different temperatures (solution

1 at 80 °C and solution 2 at room temperature). Additionally, solution 2 was sonicated for 40-50 min. Preparation conditions of the homogeneous suspensions for the coaxial electrospinning process (detailed in ESI) were the same as the uniaxial solutions 1 and 2, but without mixing them.

2.2. Fiber electrospinning

Purpose-built electrospinning equipment was employed for fibers preparation (see ESI). The solution in the shell (solution 2, electrospinning coaxial), which contained the DUT-4, had to carry PAN to give it greater viscosity and prevent the particles from being projected toward the collector. Milliliter by milliliter was also spun to prevent the particles from precipitating into the syringe. In the uniaxial conditions, the needle was set at 20 cm from the aluminum plate with a flow rate of 2.2 mL/h. The applied electrical potential difference to produce fibers was 20 kV (tips at +10 kV and collector potential at -10 kV). The coaxial conditions for both syringes were a flow rate of 0.9 mL/h, a distance of 23 cm, and an electrical potential difference was 20 kV. The fibers were stabilized at 120 ºC.

2.3. Characterization of the Fibers

The surface area and porosity of DUT-4 powders and fibers were determined by N_2 adsorption-desorption at -196 ºC (77 K), performed in a Micromeritics ASAP 2020 apparatus. Samples were outgassed at 150 ºC for at least 8 h. From the N_2 isotherm, the apparent surface area (S_{BET}) was determined by applying the Brunauer, Emmett, and Teller (BET) equation.[27] In addition, micropore volume (V_{mp}) and external surface area (S_t) were calculated by the *t*-plot method;[28] mesopore volume (V_{mes}) was obtained as the difference between the pore volume (V_p) assessed at a relative pressure close to unity (P/P_0

≈ 0.995) and the micropore volume.[29] To estimate the amount of DUT-4 in grams accessible into the fibers from the S_{BET}, the following equation was used:[30]

$$m_{DUT\text{-}4\ on\ fiber} = \frac{S_{BET}(DUT\text{-}4+fiber) - S_{BET}(PAN\ fiber)}{S_{BET}(DUT\text{-}4)} \quad (1)$$

Scanning electron microscopy (SEM) images were obtained using a JEOL JSM-6490LV microscope with acceleration voltage from 0.3 to 30 kV and a thermionic electron gun with W filament. Fourier transform infrared (FTIR) spectra were obtained from a Bruker Tensor 27 using a Golden Gate single-reflection diamond attenuated total reflection (ATR) cell to identify the functional groups on the fibers' surface, a standard spectral resolution of 4 cm^{-1} in the spectral range of 4000 to 500 cm^{-1}, were carried out. Powder X-ray diffraction (PXRD) patterns were collected in Bragg-Brentano geometry with Cu-K_α (λ = 1.54060 Å) monochromatized radiation on a PANalytical X'Pert PRO diffractometer operating with an intensity of 40 mA and a tension of 45 kV. The instrument was equipped with an X'Celerator RTMS (real-time multiple-strip) detector, and the sample patterns were recorded from 5 to 80° (2θ). Thermogravimetric analysis (TGA) was performed with a TGA 500 (TA Instruments Ltd., UK) using sample sizes of 7 to 14 mg at a heating rate of 20 °C/min from room temperature to 800 °C under an N_2 atmosphere.

2.4. Green Assessment

To quantitatively assess the greenness of DUT-4 and 70DUT-4@PAN, the free web-based DOZN™ 2.0 evaluator by MilliporeSigma was employed.[31] The software calculates the environmental impact by taking a count of the properties of raw materials, such as chemicals and solvents, including system values, such as temperature and

Journal Pre-proof

pressure.[32] The data was recollected using the UN's Globally Harmonized System of Classification and Labelling of Chemicals (GHS) and Security Data Sheet (SDS). The input data of temperature, time, pressure, and raw materials used for DOZN^{TM} 2.0 are listed in ESI.

2.5. Adsorption experiments

The adsorption experiments were carried out at 450 mg/Nm^3 of initial concentration of D4, 100 mg of adsorbent material, and room temperature. The mixtures were stirred at 700 rpm for 6–9 h to ensure equilibrium. The D4 concentration of samples was determined by gas chromatography with a flame ionization detector (GC-FID) using a Shimadzu Nexis GC-2030 (Shimadzu Corp., Kyoto, Japan). A Shimadzu SH-Rxi-5ms capillary column (15 m x 0.25 mm inner diameter x 0.25 µm film thickness) was employed. The GC-FID operational conditions were oven temperature at 110 °C; detector temperature, 250 °C; inlet temperature, 150 °C (at 83.3 kPa); carrier gas, He at a flow rate of 1.5 mL min^{-1}; splitting ratio, 5.0. An injection volume of 0.5 mL was employed with a total method duration of 1.4 min. The adsorption capacity was calculated using the mass balance in the following way:

$$q_e = \frac{(C_0 - C_e)V}{m} \qquad 2$$

where q_e is the adsorption capacity (mg/g), C_0 and C_e represent the initial and equilibrium concentration of D4 (mg/Nm^3), V is the volume of D4 solution (m^3), and m is the mass of the adsorbent (g).

2.6. Kinetic modeling

It is generally known that the adsorption kinetics of porous materials is controlled by intraparticle diffusion.[33] The homogeneous solid diffusion model (HSDM) is a typical intraparticle diffusion model, the equation is as follows:

$$\frac{\partial q}{\partial t} = \frac{D}{r^2}\frac{\partial}{\partial r}\left(r^2\frac{\partial q}{\partial r}\right) \quad (3)$$

Crank gave an exact solution to the HSDM model for the case of constant concentration at the surface (known as "infinite bath"), negligible external film resistance, and spherical adsorbent particles initially free of solute.[34] Crank's model is as follows:

$$\frac{q}{q_e} = 1 - \frac{6}{\pi^2}\sum_{n=1}^{\infty}\frac{1}{n^2}e^{\left(-\frac{Dn^2\pi^2 t}{R^2}\right)} \quad (4)$$

where q and q_e are the adsorption capacity at any time and at equilibrium, respectively (mg/g); D is the effective diffusion coefficient (m^2/h), t is the time (h), and R is the particle radius (m). This model was used to describe the kinetics of D4 siloxane onto DUT-4 powder and DUT-4 fibers and to obtain the effective diffusion coefficients.

In addition, well-known adsorption kinetics models, the pseudo-first-order model (PS-1) and the pseudo-second-order model (PS-2), were tested for the D4 siloxane adsorption, and the equations are presented as follows:

$$q = q_e(1 - e^{-K_1 t}) \quad (5)$$

$$q = \frac{K_2 q_e^2 t}{1 + K_2 q_e t} \quad (6)$$

where q and q_e are the adsorption capacity at any time and equilibrium, respectively (mg/g); K_1 *and* K_2 are the rate constants for the PS-1 and PS-2 models (h^{-1}), respectively,

188 and *t* is the time (h). The kinetic model parameters were obtained by non-linear regression
189 minimizing the standard error (Eq. 7) using the Solver add-in tool of Microsoft Excel®.
190 The goodness of fitting results was determined by the coefficient of determination (R^2).

191 $$SE = \sqrt{\frac{\sum_{i=1}^{n}(q_{exp}-q_{cal})^2}{n-k}} \quad (7)$$

192 **3. Results and discussion**

193 *3.1. Textural properties of the fibers*

194 The BET surface area of activated DUT-4 was estimated to be 1,655 m^2/g (ESI) and falls
195 well with previously reported data for this MOF.[17] The nitrogen adsorption-desorption
196 isotherms obtained at -196 ºC of the different DUT-4 fibers prepared by electrospinning are
197 type I, associated with microporous solids, independently of the electrospinning
198 configuration used (Fig. 2). These isotherms are characterized by a significant nitrogen
199 uptake at very low relative pressures. In the case of uniaxial configuration, the low volume
200 of nitrogen adsorbed at relative pressures below 0.1 shows only a limited increase of this
201 compared to the volume of nitrogen adsorbed by the PAN fiber without DUT-4. In contrast,
202 using a coaxial configuration considerably increases the volume of nitrogen adsorbed, and
203 this adsorption is directly related to the amount of DUT-4 added to the spinnable solution.
204 In addition, this coaxial configuration can also show a significant increase in the volume of
205 nitrogen adsorbed at high relative pressures, evidencing the further presence of larger
206 mesopores. Therefore, this configuration can produce DUT-4 fibers with a hierarchical
207 bimodal porous structure.

Journal Pre-proof

Table 2 collects the corresponding textural properties derived from the nitrogen adsorption-desorption isotherms obtained at -196 ºC of the DUT-4 fibers prepared by electrospinning at different configurations and experimental conditions. The coaxial configuration allowed to include not only higher amounts of DUT-4 but also reached continuous fibers with apparent surface areas as high as ~300 m^2/g. In this sense, S_{BET} values increased from 37 to 293 m^2/g as the ratio of DUT-4 to PAN enhanced; meanwhile, pore volumes, mainly associated with mesopore volumes, varied from 0.1 to 0.36 cm^3/g, suggesting the dual formation of micro and large mesopores.

The use of other solvents different than DMF was also analyzed. The calculated S_{BET} was lower for the fibers prepared with DMSO. Specifically, S_{BET} was halved with uniaxial electrospinning, while in coaxial electrospinning, S_{BET} was reduced up to four times using DMSO, so its use was discarded. Finally, it is important to highlight that although the specific surface area increases with the amount of DUT-4 added to the solution, SEM images (*vide infra*) showed DUT-4 particles of sizes larger than 1 mm on the surface of the fibers, so to optimize the dispersion of the DUT-4 particles, the use of solutions with DUT-4 percentages higher than 70% were not advisable.

From equation 1, the mass of DUT-4 accessible by nitrogen was calculated. For fibers obtained by coaxial electrospinning, the $m_{DUT\text{-}4\ on\ fiber}\ (g)$ increases following the next order: 20DUT-4@PAN (0.016) < 70DUT-4@PAN (0.062) < 100DUT-4@PAN (0.073) < 140DUT-4@PAN (0.170). However, these values represent a fraction of the initial amount of MOF on the electrospinning solution. For example, for 70DUT-4@PAN fiber, only 25%

of the initial DUT-4 mass is accessible by nitrogen suggesting the MOF is highly embedded into fibers with the formation of a thin PAN barrier coating DUT-4 particles.[35]

3.2. SEM images

Scanning electron microscopy was used to select the type of fibers that presented the best distribution of DUT-4 on the fiber surface. In Fig. 3, it can be observed that the diameters of the fibers obtained by coaxial electrospinning showed smaller diameters than those obtained by uniaxial electrospinning. The diameters for 20DUT-4@PAN, 70DUT-4@PAN, 100DUT-4@PAN, and 140DUT-4@PAN fibers were from 0.125 μm to 0.5 μm. In these types of fibers, it shows that as the amount of DUT-4 increased in the spinnable solution (*i.e.*, 20DUT-4@PAN < 70DUT-4@PAN < 100DUT-4@PAN < 140DUT-4@PAN), more particles were seen on the surface of the fiber. Furthermore, at higher DUT-4 loading fractions, particle agglomeration was observed. As a result, DUT-4 agglomerates (with an overall size >1.0 μm) were trapped between a set of fibers. Therefore, the fibers generated by 70DUT-4@PAN coaxial electrospinning had the best dispersion on the fiber surface without trapping problems.

3.3. Thermal and structural characterization of the electrospun fibers

FTIR studies of fibers are an important characterization technique to identify the functional groups on the surface material, which could be useful to explain the adsorption process on the adsorbent material. In Fig. 4, the FTIR spectra of 70DUT-4@PAN and PAN fibers are shown, the band observed at 1617.33 cm^{-1} corresponds to asymmetric stretching vibrations of the group ν_{as}(C–O),[36] the band at 991.40 cm^{-1} is associated with the bending of bridging groups δ(OH),[37] besides the 792.08 cm^{-1} band is related to flexions

into the aromatic plane;[38] the bands at 1440.69 and 1364.55 cm^{-1} can be assigned to the symmetric ν_s(OCO) stretching vibration of carboxylate group while the observed bands from 570.48 to 502.26 cm^{-1} could be associated to the stretching vibrations of the Al–O bond, in good agreement with previously reported data.[36]

To investigate the relation between PAN and DUT-4 particles in the electrospun composite fibers, PXRD measurements were performed (Fig. 5). The PXRD pattern of an as-synthesized sample of DUT-4 showed three characteristic reflections for this MOF (2θ = 6.9, 13.9, and 21.0º) corresponding to the hkl Miller index (101), (011), and (303). For polyacrylonitrile (PAN) fibers, the PXRD pattern shows an intense reflection (110) plane at 2θ = 16.8° and a weak one located at 2θ = 29.3° due to the (020) lattice plane of PAN.[39] On the other hand, the broad reflection at 2θ ≈ 25° was related to the (002) planes. These reflections are in agreement with a hexagonal chain packing of electrospun PAN-based fibers.[40] Finally, in the PXRD of 70DUT-4@PAN fibers, the characteristic diffraction peaks of both PAN and DUT-4 were observed. Therefore, the successful introduction of DUT-4 into PAN fibers can be confirmed. The two most intense reflections of DUT-4, which are related to the inorganic portion of the framework (*i.e.*, Al^{3+} distorted octahedral positions), were superimposed on the broad reflection and uneven baseline of PAN, suggesting that DUT-4 exists as crystalline material in the 70DUT-4@PAN composite.

Fig. 6(a) and 6(b) show the TGA thermograms and their derivatives of PAN fiber and 70DUT-4@PAN, respectively. For pure PAN fibers, a lower amount of absorbed water is observed at 100 °C (approximately 2.5%), and then two important weight losses can be seen. The first between 200 and 310 °C, centered at 282 °C with 30% of weight loss, and

the second change between 312 and 500 °C, centered at 430 °C representing 32% of weight loss, giving a total weight loss of 68% at 800 °C (excluding absorbed water). The TGA curve of PAN fibers has the typical thermal stability and weight loss percentages for this polymer. It has been reported that thermal changes of PAN fibers depend on the thermal processing during its manufacture (*i.e.*, stabilization temperature and processing time). If PAN was stabilized for short periods and at relatively low temperatures, a change is usually observed at 300 °C, indicating cyclization reactions with volatile gases coming out. At higher temperatures, between 320 and 480 °C, a second thermal change is typically observed and is related to a dehydrogenation reaction. Finally, in the last stage, until 700 °C, the total weight loss decreased monotonously to approximately 63%.[41] On the other hand, the sample of 70DUT-4@PAN presented higher thermal stability than alone PAN fibers with the observed changes for PAN fibers but with shifting at higher temperatures due to the presence of DUT-4, hindering chain mobility, with the first change centered at 321 °C and the second to 532 °C. However, a new change was detected at 600 °C ascribed to partial degradation of DUT-4, to give a total degradation up to 800 °C of ~64% (*i.e.*, 4% less than alone PAN fibers).

3.4. Quantitative Green Chemistry Evaluation

In addition to all physicochemical analyses, a comprehensive assessment of the environmental impact of fiber fabrication was conducted. According to green chemistry, the ideal chemical synthesis or manufacturing eliminates or reduces the waste generated, uses a negligible amount of energy, and produces no harmful products.[31] Herein, an open software (DOZN^{TM}) was used to assess the compliance with green chemistry principles (GCP) of DUT-4 and 70DUT-4@PAN (Fig. 7). Values near 0 express a minimal effect on

GCP; meanwhile, high values indicate a negative influence on GCP.[42] Minor impacts of synthesis were found in **GCP 4** (designing safer chemicals), and no significant differences were found in **GCP 8** (reduce derivatives), **GCP 9** (catalysis), and **GCP 11** (real-time analysis for pollution prevention). A major part of the impact of Principles of Green Chemistry due production of fibers was related to DUT-4 synthesis; for example, in **GCP 1** (waste prevention), the environmental score referred to DUT-4 was near 500, meanwhile, 70DUT-4@PAN was 40. Although DUT-4 synthesis and 70DUT-4@PAN used DMF as a solvent, the mass needed in synthesis was higher (28.32 g) than fibers production (6 g), and the value obtained in **GCP 1** was mainly affected by the waste severity of DMF.[31] The 90% of impacts observed in **GCP 1, GCP 2, GCP 3, GCP 5, GCP 6, GCP 7, GCP 10, and GCP 12** were produced in DUT-4 synthesis due to the waste toxic solvent. According to DOZN^{TM}, DUT-4 has an environmental score of 66, higher than the score of 1 for the fabrication of 70DUT-4@PAN fibers.

3.5. Siloxane Adsorption Performance

The adsorption experiments were carried out at an initial concentration of 450 mg/Nm^3 of siloxane D4 at room temperature. This concentration was used to be consistent with the values found in real biogas streams (*i. e.*, at low loadings). The kinetics for the adsorption of D4 was rapid, reaching equilibrium at about 3~3.5 h (Fig. 8). The adsorption capacity of the PAN fibers was tiny, 0.86 mg/g at the equilibrium concentration of 403.27 mg/m^3. The adsorption capacity for the coaxial electrospun fibers was increased from 4.13 to 8.42 mg/g at an equilibrium concentration of 256.85 to 61.26 mg/m^3, respectively.

In this sense, the fibers with the highest siloxane adsorption capacity were those electrospun coaxially, which are the fibers with the highest DUT-4 powder load and,

319 therefore, the highest S_{BET}. Although, the relationship between the siloxane adsorption
320 capacity and the specific surface area was not linear (Fig. S4). The materials obtained by
321 coaxial electrospinning achieved slight differences in the adsorption capacity. In addition,
322 the adsorption capacities obtained by coaxial fibers were only 15% lower than the DUT-4
323 powder. However, the diffusion of D4 onto coaxial fibers 20DUT-4@PAN and 70DUT-
324 4@PAN was 2.9 and 3.31-fold higher than on DUT-4 powder, based on the effective
325 diffusion coefficients obtained from Crank's model (Fig. 9). These results indicate that
326 MOF particles are fully accessible inside the polymeric fibers and that the particle
327 distribution on coaxial fibers favors the contact between the D4 siloxane and MOF
328 particles.

329 The kinetic data were fitted by the pseudo-first-order model (PS-1), pseudo-second-order
330 model (PS-2), and Crank model. The calculated model parameters and their suitability to
331 represent experimental data are shown in Table 3. Based on the high determination
332 coefficient (R^2), the kinetic adsorption of D4 on DUT-4 nanofibers can be best represented
333 by the Crank model, a well-known kinetics model based on intraparticle diffusion. These
334 results suggest that the adsorption of D4 on DUT-4 nanofibers is controlled by internal
335 mass transfer resistance, which is the common rate-limiting step for porous adsorbent
336 materials.[43]

337 Finally, the adsorption cyclability of D4 siloxane from 70DUT-4@PAN fibers by thermal
338 treatment was evaluated (see Fig. S6). For this material, a low regeneration time (~4 h)
339 was employed. Although the fibers kept their adsorption capacity showing good
340 repeatability, the complete regeneration of material under mild conditions was not
341 achieved. This behavior can be attributed to the strong interaction between D4 siloxane and

the composite fibers. The FTIR spectra of 70DUT-4@PAN before and after D4 siloxane adsorption were performed to clarify some aspects of the adsorption processes (Fig. S7). The methyl groups of the voluminous D4 molecule are expected to be mainly responsible for the adsorption complex formation. Due to this, the δ ($Si-CH_3$) band shifts to higher wavenumbers up to 1290 cm^{-1}. On the other hand, the Si−O−Si stretching band shifts to 1142 cm^{-1}. In comparison with pure D4 siloxane,[44] the position of absorption bands suggests a confinement effect. Due to the adsorption process, the material shows absorption bands with greater intensities than the original spectrum of 70DUT-4@PAN. This behavior could be attributed to the increase in the bond polarity of the functional groups of DUT-4 as a result of the strong interaction with D4 siloxane.

4. Conclusions

In summary, a novel composite from PAN and Al-MOF was successfully synthesized via electrospinning and can be used as an adsorbent to remove D4 siloxane for biogas purification applications. The coaxial electrospinning technique produced fibers with a hierarchical bimodal porous structure and superior textural characteristics compared to the uniaxial technique. Furthermore, the Al-MOF particles were well dispersed by coaxial electrospinning and were fully accessible inside the polymeric fibers. For this reason, fast adsorption kinetics was achieved (3.5 h), and the diffusion of D4 siloxane molecules was enhanced compared to DUT-4 powder. Moreover, the production of PAN fibers with DUT-4 by coaxial electrospinning had lower environmental impacts than the synthesis of the DUT-4 powder due to its low Al-MOF loadings. Taking advantage of the low environmental burden of the electrospun PAN@DUT-4 fibers and its fast kinetics, the

Journal Pre-proof

364 novel composite proposed could be of interest for the removal of D4 siloxane from gaseous
365 solutions.

366 **CRediT authorship contribution statement**

367 **Sandra Pioquinto-García:** Conceptualization, Formal analysis, Data curation,
368 Investigation. **J. Raziel Álvarez:** Formal analysis, Data curation, Writing – review &
369 editing. **Alan A. Rico-Barragán:** Data curation, Formal analysis. **Sylvain Giraudet:**
370 Formal analysis, Writing – review & editing. **Juana María Rosas-Martínez:**
371 Methodology, Formal Analysis. **Margarita Loredo-Cancino:** Validation, Formal analysis.
372 **Eduardo Soto-Regalado:** Writing – review & editing, Formal analysis. **Tomás Cordero:**
373 Formal analysis, Methodology. **José Rodríguez-Mirasol:** Conceptualization, Project
374 administration, Funding acquisition. **Nancy E. Dávila-Guzmán:** Conceptualization,
375 Writing – review & editing, Resources, Project administration, Funding acquisition.

376 **Declaration of Competing Interest**

377 The authors declare that they have no known competing financial interests or personal
378 relationships that could have appeared to influence the work reported in this paper.

379 **Acknowledgments**

380 This research was supported by Facultad de Ciencias Quimicas and Consejo Nacional de
381 Ciencia y Tecnologia de Mexico (Scholarship number 781451). J. R. Á. acknowledges
382 CONACYT for the postdoctoral fellowship (“Estancias Posdoctorales por México-2021”);
383 thanks also to J. J. Romero and R. M. Romero for many valuable discussions.

Journal Pre-proof

Appendix A. Supplementary data

Supplementary data to this article can be found online

Details of the electrospinning setup, precursor solutions, BET plots and t-plots of fibers samples, and the relationship between BET surface area and D4 adsorption capacity (PDF).

Input and output data from global greenness evaluation using DOZNTM (XLSX).

References

[1] S.N. Seo, Beyond the Paris Agreement: Climate change policy negotiations and future directions, Reg. Sci. Policy Pract. 9 (2017) 121–140. https://doi.org/10.1111/rsp3.12090.

[2] K. Obileke, N. Nwokolo, G. Makaka, P. Mukumba, H. Onyeaka, Anaerobic digestion: Technology for biogas production as a source of renewable energy—A review, Energy Environ. 32 (2021) 191–225. https://doi.org/10.1177/0958305X20923117.

[3] O.W. Awe, Y. Zhao, A. Nzihou, D.P. Minh, N. Lyczko, A Review of Biogas Utilisation, Purification and Upgrading Technologies, Waste and Biomass Valorization. 8 (2017) 267–283. https://doi.org/10.1007/s12649-016-9826-4.

[4] G. Wang, Z. Zhang, Z. Hao, Recent advances in technologies for the removal of volatile methylsiloxanes: A case in biogas purification process, Crit. Rev. Environ. Sci. Technol. 49 (2019) 2257–2313. https://doi.org/10.1080/10643389.2019.1607443.

Journal Pre-proof

[5] X.Y. Chen, H. Vinh-Thang, A.A. Ramirez, D. Rodrigue, S. Kaliaguine, Membrane gas separation technologies for biogas upgrading, RSC Adv. 5 (2015) 24399–24448. https://doi.org/10.1039/C5RA00666J.

[6] L. Ghorbel, R. Tatin, A. Couvert, Relevance of an organic solvent for absorption of siloxanes, Environ. Technol. 35 (2014) 372–382. https://doi.org/10.1080/09593330.2013.828778.

[7] J. Álvarez-Flórez, E. Egusquiza, Analysis of damage caused by siloxanes in stationary reciprocating internal combustion engines operating with landfill gas, Eng. Fail. Anal. 50 (2015) 29–38. https://doi.org/10.1016/j.engfailanal.2015.01.010.

[8] T. Jiang, W. Zhong, T. Jafari, S. Du, J. He, Y.-J. Fu, P. Singh, S.L. Suib, Siloxane D4 adsorption by mesoporous aluminosilicates, Chem. Eng. J. 289 (2016) 356–364. https://doi.org/10.1016/j.cej.2015.12.094.

[9] M. Schweigkofler, R. Niessner, Removal of siloxanes in biogases, J. Hazard. Mater. 83 (2001) 183–196. https://doi.org/10.1016/S0304-3894(00)00318-6.

[10] M. Ajhar, M. Travesset, S. Yüce, T. Melin, Siloxane removal from landfill and digester gas – A technology overview, Bioresour. Technol. 101 (2010) 2913–2923. https://doi.org/10.1016/j.biortech.2009.12.018.

[11] W. Xing, Q. Liu, J. Wang, S. Xia, L. Ma, R. Lu, Y. Zhang, Y. Huang, G. Wu, High Selectivity and Reusability of Biomass-Based Adsorbent for Chloramphenicol Removal, Nanomaterials. 11 (2021) 2950. https://doi.org/10.3390/nano11112950.

Journal Pre-proof

[12] Y. Mito-oka, S. Horike, Y. Nishitani, T. Masumori, M. Inukai, Y. Hijikata, S. Kitagawa, Siloxane D4 capture by hydrophobic microporous materials, J. Mater. Chem. A. 1 (2013) 7885–7888. https://doi.org/10.1039/c3ta11217a.

[13] A. Peluso, N. Gargiulo, P. Aprea, F. Pepe, D. Caputo, Nanoporous Materials as H2S Adsorbents for Biogas Purification: a Review, Sep. Purif. Rev. 48 (2019) 78–89. https://doi.org/10.1080/15422119.2018.1476978.

[14] T. Saeed, A. Naeem, I. Ud Din, M.A. Alotaibi, A.I. Alharthi, I. Wali Khan, N. Huma Khan, T. Malik, Structure, nomenclature and viable synthesis of micro/nanoscale metal organic frameworks and their remarkable applications in adsorption of organic pollutants, Microchem. J. 159 (2020) 105579. https://doi.org/10.1016/j.microc.2020.105579.

[15] M. Sánchez-Serratos, J.R. Álvarez, E. González-Zamora, I.A. Ibarra, Porous Coordination Polymers (PCPs): New Platforms for Gas Storage, J. Mex. Chem. Soc. 60 (2016) 43–57.

[16] L. Öhrström, Let's talk about MOFs—Topology and terminology of metal-organic frameworks and why we need them, Crystals. 5 (2015) 154–162. https://doi.org/10.3390/cryst5010154.

[17] E. Gulcay, P. Iacomi, Y. Ko, J.S. Chang, G. Rioland, S. Devautour-Vinot, G. Maurin, Breaking the upper bound of siloxane uptake: metal–organic frameworks as an adsorbent platform, J. Mater. Chem. A. 9 (2021) 12711–12720. https://doi.org/10.1039/D1TA02275J.

Journal Pre-proof

[18] I. Senkovska, F. Hoffmann, M. Fröba, J. Getzschmann, W. Böhlmann, S. Kaskel, New highly porous aluminium based metal-organic frameworks: Al(OH)(ndc) (ndc = 2,6-naphthalene dicarboxylate) and Al(OH)(bpdc) (bpdc = 4,4′-biphenyl dicarboxylate), Microporous Mesoporous Mater. 122 (2009) 93–98. https://doi.org/10.1016/j.micromeso.2009.02.020.

[19] J.E. Efome, D. Rana, T. Matsuura, C.Q. Lan, Insight Studies on Metal-Organic Framework Nanofibrous Membrane Adsorption and Activation for Heavy Metal Ions Removal from Aqueous Solution, ACS Appl. Mater. Interfaces. 10 (2018) 18619–18629. https://doi.org/10.1021/acsami.8b01454.

[20] K.-L. Chiu, F. Kwong, D.H.L. Ng, Enhanced oxidation of CO by using a porous biomorphic CuO/CeO2/Al2O3 compound, Microporous Mesoporous Mater. 156 (2012) 1–6. https://doi.org/10.1016/j.micromeso.2012.02.015.

[21] K.-L. Chiu, D.H.L. Ng, Synthesis and characterization of cotton-made activated carbon fiber and its adsorption of methylene blue in water treatment, Biomass and Bioenergy. 46 (2012) 102–110. https://doi.org/10.1016/j.biombioe.2012.09.023.

[22] Z. Zhang, J. Li, F. Sun, D. H. L. Ng, F. Kwong, S. Liu, Preparation and Characterization of Activated Carbon Fiber from Paper, Chinese J. Chem. Phys. 24 (2011) 103–108. https://doi.org/10.1088/1674-0068/24/01/103-108.

[23] D. Han, A.J. Steckl, Coaxial Electrospinning Formation of Complex Polymer Fibers and their Applications, Chempluschem. 84 (2019) 1453–1497. https://doi.org/10.1002/cplu.201900281.

Journal Pre-proof

[24] R. Ostermann, J. Cravillon, C. Weidmann, M. Wiebcke, B.M. Smarsly, Metal-organic framework nanofibers via electrospinning, Chem. Commun. 47 (2011) 442–444. https://doi.org/10.1039/c0cc02271c.

[25] J. Ren, N.M. Musyoka, P. Annamalai, H.W. Langmi, B.C. North, M. Mathe, Electrospun MOF nanofibers as hydrogen storage media, Int. J. Hydrogen Energy. 40 (2015) 9382–9387. https://doi.org/10.1016/j.ijhydene.2015.05.088.

[26] S. Pioquinto-García, J.M. Rosas, M. Loredo-Cancino, S. Giraudet, E. Soto-Regalado, P. Rivas-García, N.E. Dávila-Guzmán, Environmental assessment of metal-organic framework DUT-4 synthesis and its application for siloxane removal, J. Environ. Chem. Eng. 9 (2021) 106601. https://doi.org/10.1016/j.jece.2021.106601.

[27] S. Brunauer, P.H. Emmett, E. Teller, Adsorption of Gases in Multimolecular Layers, J. Am. Chem. Soc. 60 (1938) 309–319. https://doi.org/citeulike-article-id:4074706\rdoi: 10.1021/ja01269a023.

[28] W.D. Harkins, G. Jura, Surfaces of Solids. XIII. A Vapor Adsorption Method for the Determination of the Area of a Solid without the Assumption of a Molecular Area, and the Areas Occupied by Nitrogen and Other Molecules on the Surface of a Solid, J. Am. Chem. Soc. 66 (1944) 1366–1373. https://doi.org/10.1021/ja01236a048.

[29] M. Thommes, K. Kaneko, A. V. Neimark, J.P. Olivier, F. Rodriguez-Reinoso, J. Rouquerol, K.S.W. Sing, Physisorption of gases, with special reference to the evaluation of surface area and pore size distribution (IUPAC Technical Report), Pure Appl. Chem. 87 (2015) 1051–1069. https://doi.org/10.1515/pac-2014-1117.

Journal Pre-proof

[30] G.W. Peterson, D.T. Lee, H.F. Barton, T.H. Epps, G.N. Parsons, Fibre-based composites from the integration of metal–organic frameworks and polymers, Nat. Rev. Mater. 6 (2021) 605–621. https://doi.org/10.1038/s41578-021-00291-2.

[31] A. DeVierno Kreuder, T. House-Knight, J. Whitford, E. Ponnusamy, P. Miller, N. Jesse, R. Rodenborn, S. Sayag, M. Gebel, I. Aped, I. Sharfstein, E. Manaster, I. Ergaz, A. Harris, L. Nelowet Grice, A Method for Assessing Greener Alternatives between Chemical Products Following the 12 Principles of Green Chemistry, ACS Sustain. Chem. Eng. 5 (2017) 2927–2935. https://doi.org/10.1021/acssuschemeng.6b02399.

[32] C. Brambila, P. Boyd, A. Keegan, P. Sharma, C. Vetter, E. Ponnusamy, S. V. Patwardhan, A Comparison of Environmental Impact of Various Silicas Using a Green Chemistry Evaluator, ACS Sustain. Chem. Eng. 10 (2022) 5288–5298. https://doi.org/10.1021/acssuschemeng.2c00519.

[33] J. Liu, H. Cao, Y. Shi, P. Jiang, Enhanced Methane Delivery in MIL-101(Cr) by Means of Subambient Cooling, Energy & Fuels. 35 (2021) 6898–6908. https://doi.org/10.1021/acs.energyfuels.1c00617.

[34] J. Crank, The Mathematics of Diffusion, Clarendon Press, Oxford, 1979. https://books.google.com.mx/books?id=eHANhZwVouYC.

[35] M. Armstrong, P. Sirous, B. Shan, R. Wang, C. Zhong, J. Liu, B. Mu, Prolonged HKUST-1 functionality under extreme hydrothermal conditions by electrospinning polystyrene fibers as a new coating method, Microporous Mesoporous Mater. 270

Journal Pre-proof

(2018) 34–39. https://doi.org/10.1016/j.micromeso.2018.05.004.

[36] J.F. Kurisingal, Y. Li, Y. Sagynbayeva, R.K. Chitumalla, S. Vuppala, Y. Rachuri, Y. Gu, J. Jang, D.-W. Park, Porous aluminum-based DUT metal-organic frameworks for the transformation of CO2 into cyclic carbonates: A computationally supported study, Catal. Today. 352 (2020) 227–236. https://doi.org/10.1016/j.cattod.2019.12.038.

[37] H. Embrechts, M. Kriesten, M. Ermer, W. Peukert, M. Hartmann, M. Distaso, In situ Raman and FTIR spectroscopic study on the formation of the isomers MIL-68(Al) and MIL-53(Al), RSC Adv. 10 (2020) 7336–7348. https://doi.org/10.1039/C9RA09968A.

[38] E. Pretsch, P. Bühlmann, M. Badertscher, IR Spectroscopy, in: Struct. Determ. Org. Compd., Springer-Verlag, Berlin, Heidelberg, 2009: pp. 1–67. https://doi.org/10.1007/978-3-540-93810-1_7.

[39] Y. Zhang, N. Tajaddod, K. Song, M.L. Minus, Low temperature graphitization of interphase polyacrylonitrile (PAN), Carbon N. Y. 91 (2015) 479–493. https://doi.org/10.1016/j.carbon.2015.04.088.

[40] X. Hu, D.J. Johnson, J.G. Tomka, Molecular Modelling of the Structure of Polyacrylonitrile Fibres, J. Text. Inst. 86 (1995) 322–331. https://doi.org/10.1080/00405009508631337.

[41] S. Lee, J. Kim, B.-C. Ku, J. Kim, H.-I. Joh, Structural Evolution of Polyacrylonitrile Fibers in Stabilization and Carbonization, Adv. Chem. Eng. Sci. 02 (2012) 275–282.

Journal Pre-proof

https://doi.org/10.4236/aces.2012.22032.

[42] P. Sharma, C. Vetter, E. Ponnusamy, E. Colacino, Assessing the Greenness of Mechanochemical Processes with the DOZN 2.0 Tool, ACS Sustain. Chem. Eng. 10 (2022) 5110–5116. https://doi.org/10.1021/acssuschemeng.1c07981.

[43] J. Kärger, D.M. Ruthven, D.N. Theodorou, Sorption Kinetics, in: Diffus. Nanoporous Mater., Wiley, 2012: pp. 143–189. https://doi.org/10.1002/9783527651276.ch6.

[44] V.T.L. Tran, P. Gélin, C. Ferronato, J. Chovelon, L. Fine, G. Postole, Adsorption of linear and cyclic siloxanes on activated carbons for biogas purification: Sorbents regenerability, Chem. Eng. J. 378 (2019) 122152. https://doi.org/10.1016/j.cej.2019.122152.

Journal Pre-proof

Tables

Table 1. Details of each electrospinning solution employed.

Notation	Solution 1		Solution 2			Electrospinning operational mode
	PAN (g)	DMF (g)	DUT-4 (g)	DMF (g)	PAN (g)	
PAN	0.3	3.0	N/A[a]	N/A	N/A	Uniaxial
20DUT-4/PAN	0.5	2.0	0.1	3.0	N/A	Uniaxial
20DUT-4@PAN	0.4	2.5	0.1	2.5	0.1	Coaxial
70DUT-4@PAN	0.25	3.0	0.25	3.0	0.1	Coaxial
100DUT-4@PAN	0.25	3.0	0.35	3.0	0.1	Coaxial
140DUT-4@PAN	0.25	3.0	0.50	3.0	0.1	Coaxial

[a]N/A: not applicable

Table 2. Textural properties derived from the nitrogen adsorption-desorption isotherms obtained at -196 ºC of the DUT-4 fibers.

Fiber notation	S_{BET} (m^2/g)	V_{mp} (cm^3/g)	S_t (m^2/g)	V_{mes} (cm^3/g)	V_p (cm^3/g)
PAN	11	0.002	6	0.025	0.027
20DUT-4/PAN	20	0.004	10	0.055	0.059
20DUT-4@PAN	37	0.010	13	0.090	0.100
70DUT-4@PAN	113	0.033	33	0.188	0.221
100DUT-4@PAN	131	0.040	35	0.120	0.160
140DUT-4@PAN	293	0.100	51	0.264	0.363

Table 3. Kinetic model parameters for siloxane D4 adsorption.

Adsorbent	PS-1		PS-2		Crank	
	K_1 (h^{-1})	R^2	K_2 (h^{-1})	R^2	D (m^2/h)	R^2
DUT-4	1.14	0.9456	0.22	0.9231	$1.76x10^{-8}$	0.9768
20DUT-4/PAN	6.43	0.9917	2.13	0.9977	$4.22x10^{-8}$	0.9921
20DUT-4@PAN	5.87	0.9671	1.18	0.9840	$5.12x10^{-8}$	0.9780
70DUT-4@PAN	5.33	0.8810	0.76	0.9736	$5.82x10^{-8}$	0.9530
100DUT-4@PAN	2.59	0.9692	0.61	0.9463	$3.32x10^{-8}$	0.9823

140DUT-4@PAN	2.59	0.9460	0.38	0.9860	$3.32x10^{-8}$	0.9936

551

Journal Pre-proof

552 **Figure captions**

553 **Fig. 1.** Crystal structure of DUT-4. (A) the aluminum octahedra are linked by NDC groups,
554 (B) view of the rectangular tunnels (9 Å × 9 Å) along the [010] direction. Color code: gray,
555 C; red, O; blue polyhedral, Al.

556 **Fig. 2.** Nitrogen adsorption-desorption isotherms obtained at -196 ºC of the DUT-4 fibers
557 prepared by uniaxial (a) and coaxial (b) electrospinning configuration at different
558 experimental conditions.

559 **Fig. 3.** SEM micrographs of electrospun fibers: (A) PAN, (B) 20DUT-4/PAN, (C) 20DUT-
560 4@PAN, (D) 70DUT-4@PAN, (E) 100DUT-4@PAN, (F) 140DUT-4@PAN.

561 **Fig. 4.** ATR-FTIR spectra of the pristine DUT-4 and the fibers (PAN and 70DUT-
562 4@PAN).

563 **Fig. 5.** PXRD patterns of (a) simulated DUT-4, (b) as-synthesized DUT-4 powders, (c)
564 electrospun DUT-4 powders-embedded fibers (70DUT-4@PAN), and (d) PAN fibers. The
565 insert presents the chain packing of PAN in [110] direction.

566 **Fig. 6.** (A) TGA and (B) DTG curves of PAN and 70DUT-4@PAN fibers.

567 **Fig. 7.** Green Assessment of DUT-4 and 70DUT-4@PAN.

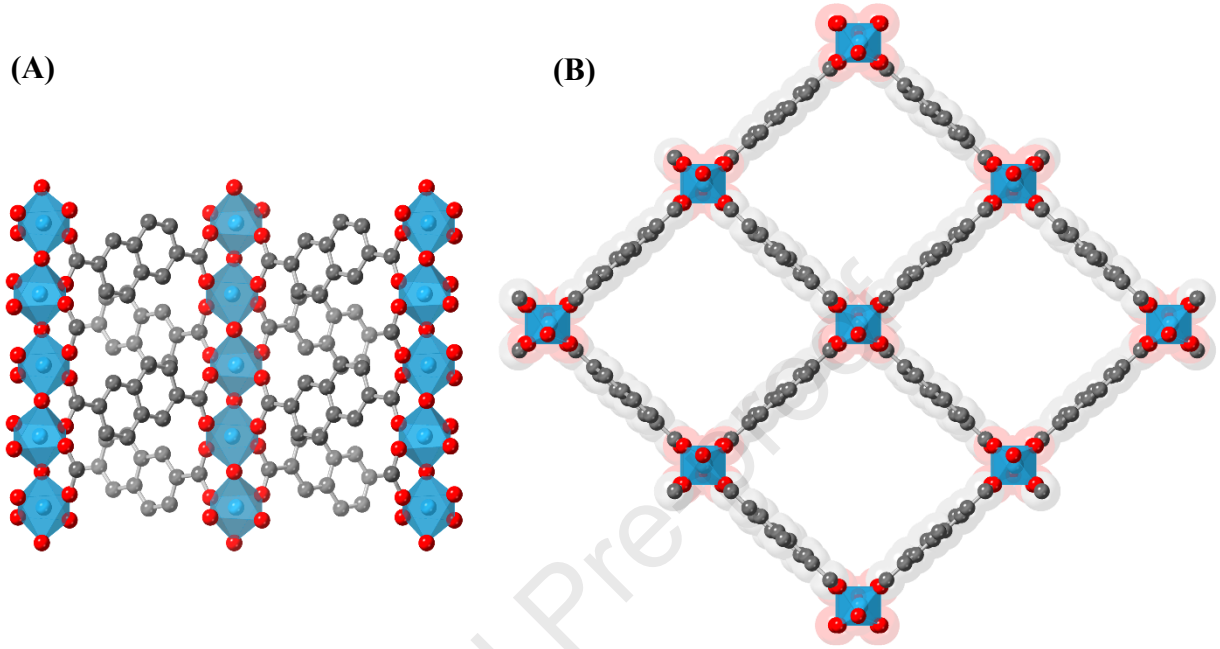
568 **Fig. 8.** Adsorption kinetics profiles of electrospun DUT-4 fibers at room temperature and
569 initial D4 concentration of 450 mg/Nm^3.

570 **Fig. 9.** Effective diffusion coefficients for D4 siloxane adsorption at 450 mg/Nm^3 and room
571 temperature.

Journal Pre-proof

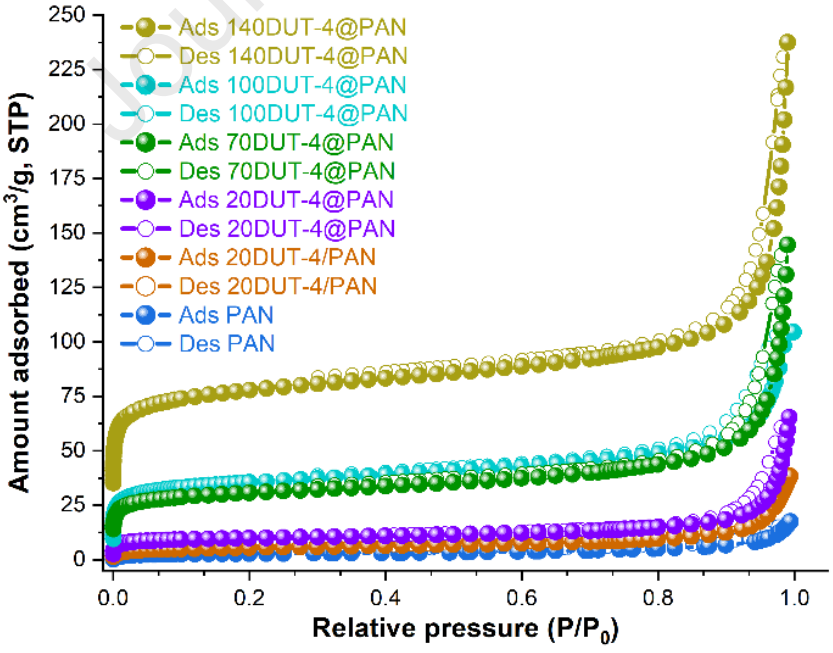
572 **Figures**

573 **Figure 1**



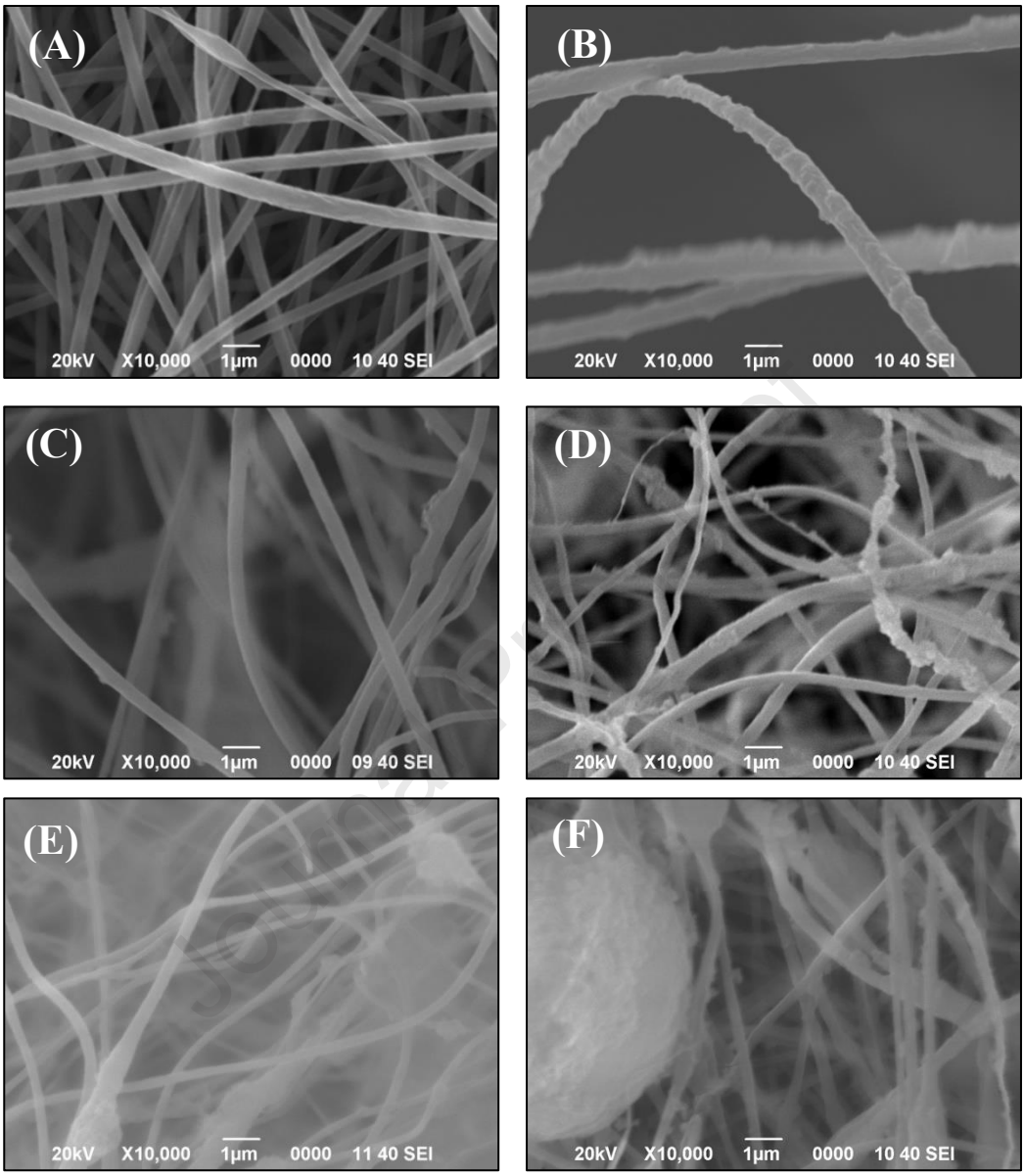
574

575 **Figure 2**



576

577 **Figure 3**



578

579

Figure 4

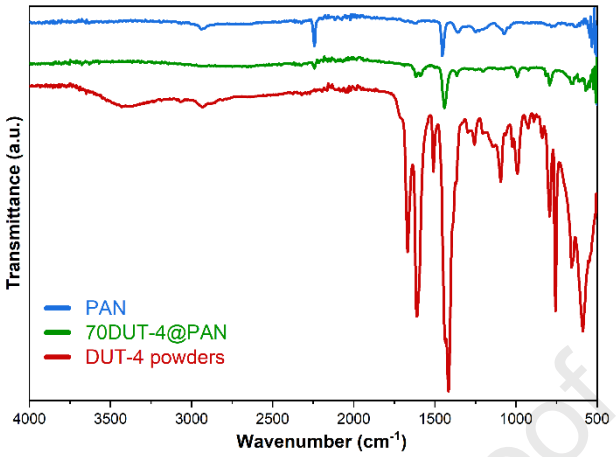
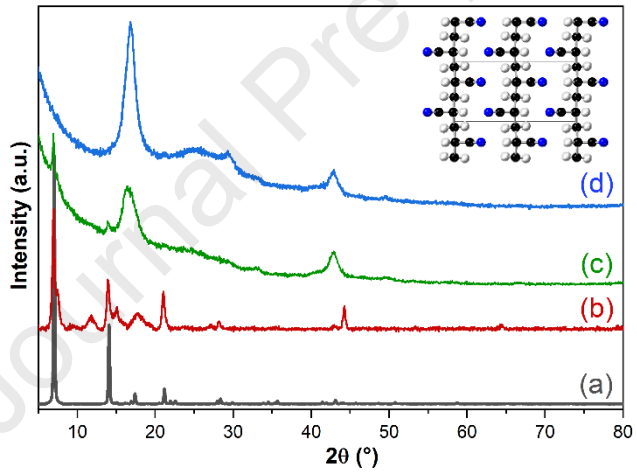
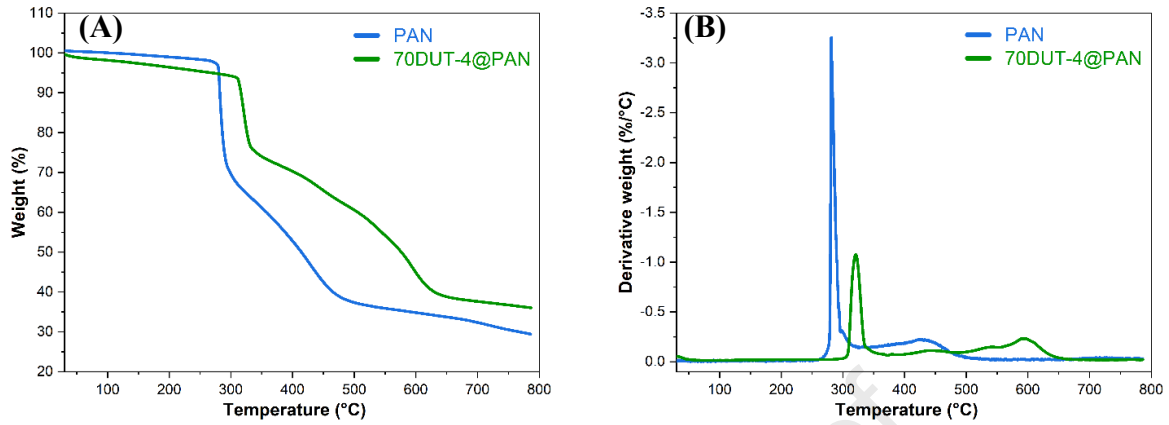


Figure 5



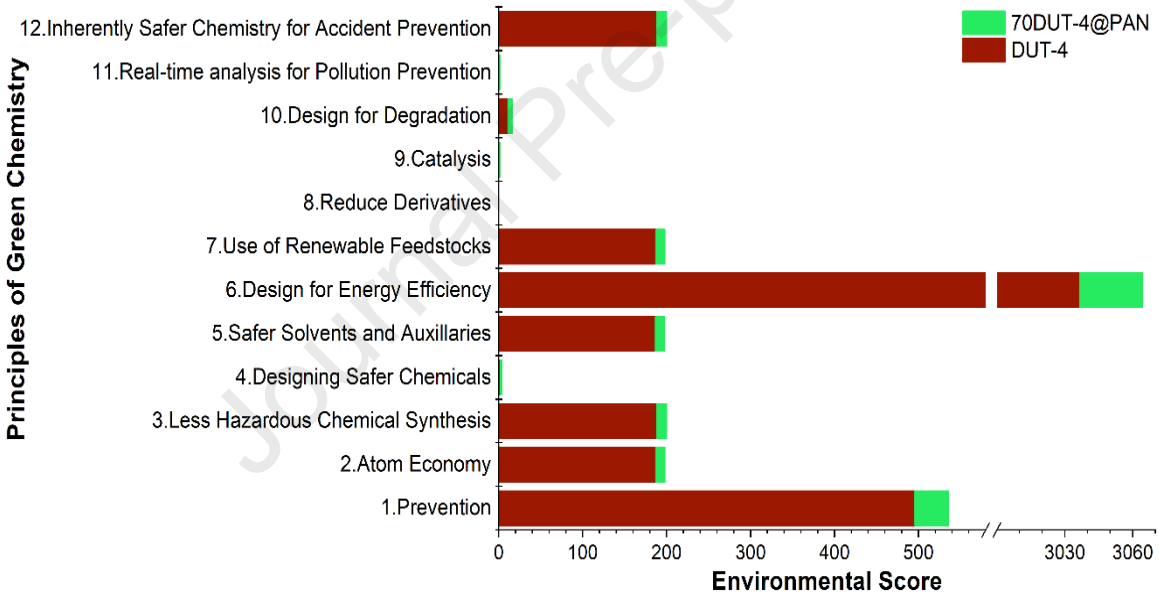
Journal Pre-proof

589 **Figure 6**



590
591

592 **Figure 7**



593

Journal Pre-proof

Figure 8

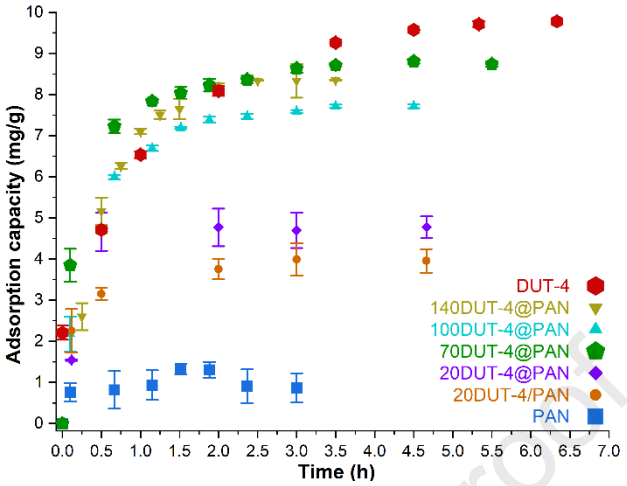
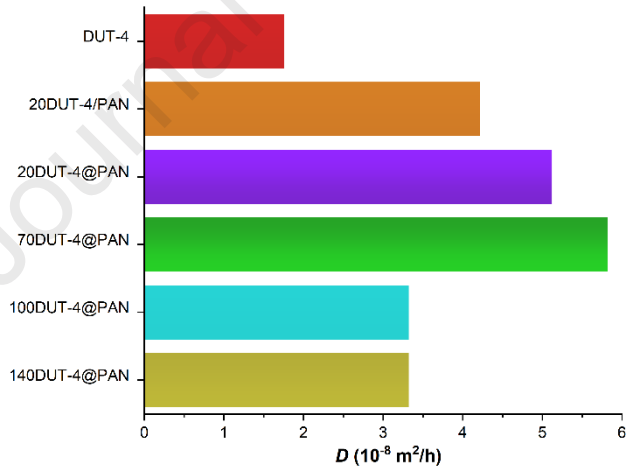


Figure 9



Journal Pre-proof

- Aluminum-based MOF/PAN composite fibers were prepared by electrospinning
- Coaxial electrospun fibers show superior textural characteristics
- The fibers can be used to adsorb siloxane D4 at low concentrations
- 70DUT-4@PAN has the best relation between adsorption kinetics/environmental impact

Journal Pre-proof

Journal Pre-proof

Declaration of interests

☒ The authors declare that they have no known competing financial interests or personal relationships that could have appeared to influence the work reported in this paper.

☐The authors declare the following financial interests/personal relationships which may be considered as potential competing interests:

Journal Pre-proof